OPTIMIZING MATERIAL DISTRIBUTION FOR PRESCRIBED APPARENT FRACTURE TOUGHNESS IN FGM COATINGS

Ali Mohammad Afsar *
Department of Mechanical Engineering, Bangladesh University of Engineering and Technology, Dhaka 1000, Bangladesh
Hideki Sekine
Department of Aeronautics and Space Engineering, Tohoku University, Aoba-yama 01, Aoba-ku, Sendai 980-8579, Japan

Abstract This paper is concerned with the inverse problem of optimizing material distribution with a view to realizing prescribed apparent fracture toughness in Functionally Graded Material (FGM) coatings. The incompatible eigenstrain induced in the FGM coatings after cooling from the sintering temperature due to mismatch in the coefficients of thermal expansion is taken into consideration. Simulating the nonhomogeneous material properties of the FGM coatings by an equivalent eigenstrain, we present an approximation method of calculating stress intensity factor (SIF) for an edge crack in the FGM coatings. The approximation method of the SIF is used in the inverse problem of optimizing material distribution intending to realize prescribed apparent fracture toughness in the FGM coatings. Numerical results obtained for a TiC/Al_2O_3 FGM coating-Al_2O_3 substrate reveal that the apparent fracture toughness significantly depends on the material distribution, and can be controlled within possible limits by choosing an optimum material distribution profile

Keyword: Composite material, Inverse problem, Functionally graded material, Fracture toughness

INTRODUCTION

Functionally graded materials (FGMs) consist of two or more distinct material phases and have a distinguished feature that the material distributions and microstructures of these materials continuously vary along the space variables. This feature provides the FGMs with outstanding advantages over homogeneous materials and conventional composite materials. From a mechanics viewpoint the main advantages of material property grading appear to be improved bonding strength, toughness, and wear and corrosion resistance, and reduced residual and thermal stresses. Therefore, FGM coatings have wide applications in automotive engines, and cutting and grinding tools to protect the surfaces from melting, wear, corrosion and oxidation. However, in FGM coatings, cracks perpendicular to the coating surface can initiate and propagate into the coating under applied thermal or mechanical tensile loads. [1]Further, Gecit,[2] and Hu and Evans [3] reported that multiple cracking in the coating is a common damage mechanism in many coating/substrate systems. Thus it is of great importance to design the FGM coatings so that they can have higher fracture strength.

The design of FGMs invokes the inverse problem by which an optimum material distribution profile can be determined to realize a prescribed characteristic in FGMs for high performance and efficiency in practical working conditions. Markworth and Saunders[1] considered the inverse problem to optimize an assumed functional form for the spatially dependent material distribution subject to certain constraints such as maximizing or minimizing the heat flux across the material. Further references of inverse problems of designing FGMs with various geometries subject to various constraints can be found in [5-7]

The inverse problems mentioned above concentrated on the design of FGMs to obtain desired thermal characteristics. To obtain desired fracture characteristics in FGMs, the analytical solution to the inverse problem of material distribution profiles turns to be very complicated due to their nonhomogeneous material properties. In addition, the incompatible eigenstrain induced in these materials after cooling from the sintering temperature due to mismatch in the coefficients of thermal expansion is to be considered since it has a great influence on their fracture characteristics. Sekine and Afsar [8], and Afsar and Sekine[9]considered the inverse problems of material distribution profiles to obtain desired brittle fracture characteristics in semi-infinite FGMs with arbitrary variation of material properties for the case of a

*Email: mafsaral@me.buet.edu

single and periodic edge cracks, respectively.

In this paper, we concentrate on the inverse problem of optimizing material distribution intending to realize prescribed apparent fracture toughness in FGM coatings. We introduce an approximation method of calculating SIFs for an edge crack in the FGM coatings with arbitrary variation of material properties. The approximation method of SIFs is applied to the inverse calculation of optimum material distributions intending to realize prescribed apparent fracture toughness in the FGM coatings.

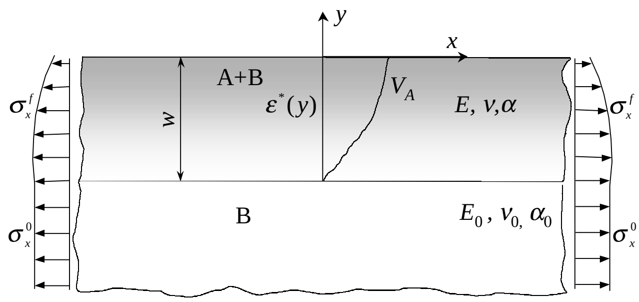

Fig. 1 Analytical model of an FGM coating perfectly bonded to a semi-infinite homogeneous elastic

MODELING OF FGM COATINGS

Let us consider an FGM coating perfectly bonded to a semi-infinite homogeneous elastic substrate as shown in Fig. 1. The origin of the Cartesian coordinate system *x*-*y* is located at the coating surface. The FGM coating of finite thickness *w* is composed of two constituents A and B, and their volume fractions V_A and V_B vary in the *y* direction only. The constituent of the substrate is B. The Young's modulus, Poisson's ratio and the coefficient of thermal expansion of the coating region are denoted by E, ν and α, respectively, while the corresponding properties of the homogeneous substrate are designated by E_0, ν_0 and α_0. When such a composite is fabricated and cooled after processing, an incompatible eigenstrain is induced in the FGM coating, which is given by

$$\varepsilon^* = (\alpha_0 - \alpha)\Delta T \, , \qquad (1)$$

where ΔT is the difference in the processing and room temperatures. Since the FGM coating is assumed to be isotropic, the components of the incompatible eigenstrain are equal. For this model of the FGM coating in plane strain condition, we carry out inverse calculations of material distributions intending to realize prescribed apparent fracture toughness in the FGM coating subjected to a far-field applied load.

INVERSE ANALYSIS OF BRITTLE FRACTURE CHARACTERISTICS

FGMs are nonhomogeneous solids and, therefore, their nonhomogeneities have to be considered in studying the fracture characteristics of these materials. The consideration of these nonhomogeneities complicates the analytical studies due to mathematical difficulties. Thus it is often conventional to regard the material properties to be some certain assumed functions of space variable, for instance, exponential and power functions, in order to simplify the problems. However, in the inverse design of FGMs, in which material distribution profiles have to be determined to achieve desired fracture characteristics, special functional forms of the properties cannot be assumed, since these assumed functional forms of the properties may not be physically realizable for some materialdistribution profiles obtained by inverse calculations. Therefore, as an alternate approach, an approximation method is used in this study to calculate SIFs for a crack in FGM coatings and is employed in the inverse problem of calculating material distribution profiles in FGM coatings intending to realize prescribed fracture characteristics.

Approximation method of SIF

In the approximation method of SIFs, we first homogenize the FGM coating by simulating the material nonhomogeneities by a distribution of equivalent eigenstrain. The distribution of the equivalent eigenstrain to be determined is such that the elastic fields are identical in both the FGM and the homogenized coatings under the same loading conditions. After determining the distribution of the equivalent eigenstrain, a method is formulated to calculate SIFs for a crack in the homogenized coatings subjected to external loadings. Since the equivalent eigenstrain is determined from the condition of identical elastic fields in the uncracked FGM and homogenized coatings, the elastic filed in the cracked homogenized coatings cannot exactly represent the elastic field in the cracked FGM coatings. However, the validity of the approximation method is within acceptable limits as discussed in our previous work [8].

As stated earlier, the equivalent eigenstrain is determined from the condition of identical elastic fields in the uncracked FGM and homogenized coatings subjected to the same loading condition. To determine the elastic field, we first consider an FGM coating bonded to a semi-infinite substrate subjected to the far-field tensile stress as shown in Fig. 1. As given by Eq. (1), an incompatible eigenstrain $\varepsilon^*(y)$, which is a function of *y* only, is induced in the FGM coating. The resultant elastic field in this coating is obtained by superposing the elastic field induced by the incompatible eigenstrain $\varepsilon^*(y)$ and that developed due to the applied stress. The elastic field in the FGM coating due to the applied stress can be derived as

$$\sigma_x = \frac{1-\nu_0^2}{1-\nu^2}\frac{E}{E_0}\sigma_x^0\,,\quad \sigma_z = \frac{\nu(1-\nu_0^2)}{1-\nu^2}\frac{E}{E_0}\sigma_x^0\,,$$
$$\varepsilon_x = \frac{1-\nu_0^2}{E_0}\sigma_x^0\,,\quad \varepsilon_y = -\frac{\nu(1-\nu_0^2)}{1-\nu}\frac{\sigma_x^0}{E_0}. \tag{2}$$

In deriving Eq. (2), it is assumed that σ_y = 0 and the strain component ε_x in the coating is equal to that in the substrate under the uniform stress σ_x^0, since the thickness *w* of the FGM coating is small in comparison with that of the substrate. To obtain the elastic field due to the incompatible eigenstrain, we have the following stress-strain relations:

$$\varepsilon_x = \frac{1}{E}\left(\sigma_x - \nu\sigma_y - \nu\sigma_z\right) + \varepsilon^*,$$
$$\varepsilon_y = \frac{1}{E}\left(\sigma_y - \nu\sigma_x - \nu\sigma_z\right) + \varepsilon^*, \tag{3}$$
$$\varepsilon_z = \frac{1}{E}\left(\sigma_z - \nu\sigma_x - \nu\sigma_y\right) + \varepsilon^*.$$

In plane strain condition, ε_z = 0 and also as before σ_y = 0. Again, it is noted that the thickness *w* is small. Therefore, the total strain in the *x* and *y* directions will be completely suppressed by the restraining effect from the substrate. Thus we obtain

$$\sigma_x = -\frac{E}{1-\nu}\varepsilon^*\,,\quad \sigma_z = -\frac{E}{1-\nu}\varepsilon^*\,,$$
$$\varepsilon_x = 0\,,\quad \varepsilon_y = \frac{1+\nu}{1-\nu}\varepsilon^*. \tag{4}$$

The resultant field in the FGM coating is thus written as

$$\sigma_x^f = \frac{1-\nu_0^2}{1-\nu^2}\frac{E}{E_0}\sigma_x^0 - \frac{E}{1-\nu}\varepsilon^*\,,\quad \sigma_y^f = 0\,,$$
$$\sigma_z^f = \frac{\nu(1-\nu_0^2)}{1-\nu^2}\frac{E}{E_0}\sigma_x^0 - \frac{E}{1-\nu}\varepsilon^*, \tag{5}$$

$$\varepsilon_x^f = \frac{1-\nu_0^2}{E_0}\sigma_x^0\,,\quad \varepsilon_y^f = -\frac{\nu(1-\nu_0^2)}{1-\nu}\frac{\sigma_x^0}{E_0} + \frac{1+\nu}{1-\nu}\varepsilon^*\,, \tag{6}$$
$$\varepsilon_z^f = 0.$$

Now we consider a semi-infinite homogeneous medium consisting of material B with the same geometry as shown in Fig. 1. In addition to the far-field uniform applied stress σ_x^0, the corresponding FGM coating region of this medium is assumed to have the same incompatible eigenstrain $\varepsilon^*(y)$. The resultant elastic field in the corresponding FGM coating region for this case can be readily derived as

$$\sigma_x^{h0} = \sigma_x^0 - \frac{E_0}{1-\nu_0}\varepsilon^*\,,\quad \sigma_y^{h0} = 0\,,$$
$$\sigma_z^{h0} = \nu_0\sigma_x^0 - \frac{E_0}{1-\nu_0}\varepsilon^*\,,$$

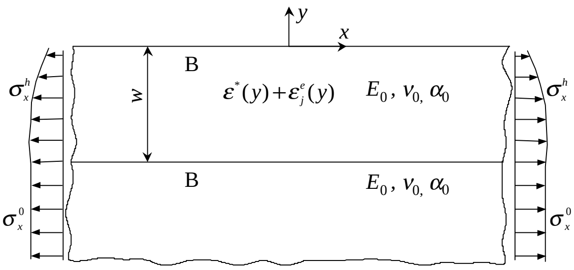

Fig. 2 Semi-infinite homogeneous medium with a distribution of incompatible and equivalent eigenstrains in the coating region

Now let us consider a distribution of equivalent eigenstrain ε_i^e, where *i* = *x*, *y*, and *z*, in the corresponding FGM coating region of the semi-infinite homogeneous medium such that the elastic fields in the FGM coating regions become identical. Thus we can write

$$\sigma_x^f = \sigma_x^{h0} + \sigma_x^e,\quad \sigma_y^f = \sigma_y^{h0} + \sigma_y^e,\quad \sigma_z^f = \sigma_z^{h0} + \sigma_z^e,$$
$$\varepsilon_x^f = \varepsilon_x^{h0} + e_x + \varepsilon_x^e,\quad \varepsilon_y^f = \varepsilon_y^{h0} + e_y + \varepsilon_y^e, \tag{9}$$
$$\varepsilon_z^f = \varepsilon_z^{h0} + e_z + \varepsilon_z^e,$$

where σ_i^e and e_i, respectively, represent the stress and elastic strain arising due to the equivalent eigenstrain ε_i^e. Noting that e_i is related to σ_i^e by Hooke's law and using Eqs.(5) through (9) we obtain the expressions for equivalent eigenstrains as

$$\varepsilon_x^e = \left[1 - \frac{1-\nu\nu_0}{1-\nu^2}\frac{E}{E_0}\right]\frac{1-\nu_0^2}{E_0}\sigma_x^0 + \left[\frac{E}{1-\nu} - \frac{E_0}{1-\nu_0}\right]\frac{1-\nu_0}{E_0}\varepsilon^*,$$
$$\varepsilon_y^e = \left[\nu\nu_0 - \nu - \nu^2 + \frac{\nu_0 E}{E_0}\right]\frac{1-\nu_0^2}{1-\nu^2}\frac{\sigma_x^0}{E_0} + \left[\nu - \nu_0\frac{E}{E_0}\right]\frac{2\varepsilon^*}{1-\nu},$$
$$\varepsilon_z^e = \frac{(1-\nu_0^2)(\nu_0-\nu)}{1-\nu^2}\frac{E}{E_0}\frac{\sigma_x^0}{E_0} + \left[\frac{E}{1-\nu} - \frac{E_0}{1-\nu_0}\right]\frac{1-\nu_0}{E_0}\varepsilon^*, \tag{10}$$

and the resultant stress components in the semi-infinite homogeneous medium are derived as

$$\sigma_x^h = \frac{\Delta T E}{1-\nu}(\alpha-\alpha_0) + \left[\frac{1-\nu_0^2}{1-\nu^2}\frac{E}{E_0} - 1\right]\sigma_x^0 + \sigma_x^0\,,$$
$$\sigma_z^h = \frac{\Delta T E}{1-\nu}(\alpha-\alpha_0) + \left[\frac{\nu(1-\nu_0^2)}{1-\nu^2}\frac{E}{E_0} - \nu_0\right]\sigma_x^0 + \sigma_x^0. \tag{11}$$

The other stress component is zero.

Fig.2 shows the semi-infinite homogeneous medium with distributed incompatible and equivalent eigenstrains in the coating region under the far-field tensile stress, which is obtained by homogenizing the

FGM coating/substrate system shown in Fig. 1. Now suppose that the semi-infinite homogeneous medium in Fig. 2 contains an edge crack of length l as shown

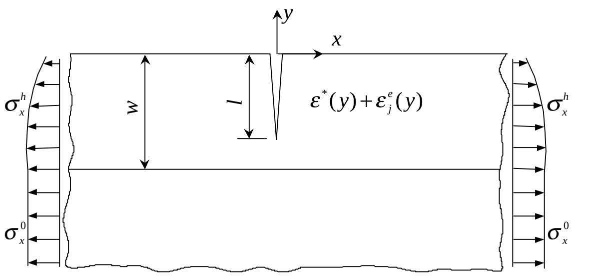

Fig. 3 An edge crack in a semi-infinite homogeneous medium with distributed incompatible and equivalent eigenstrains in the

in Fig. 3. For this crack, we can obtain a singular integral equation replacing the crack by a continuous distribution of edge dislocations and can be converted to a system of algebraic equations to determine the unknown density function $\varphi_x(T_s)$ as follows

$$\frac{2\mu_0}{(\kappa_0+1)}\left[\sum_{s=1}^{N}\varphi_x(T_s)(1+T_s)\left\{\frac{1}{H_q-T_s}+k(H_q,T_s)\right\}\right] = -\frac{2N+1}{2}\left[\sigma_x^h(H_q)\right]; \quad q=1,2,3,...,N. \tag{12}$$

Here, the collocation and integration points are given by

$$H_q=\cos\left(\frac{2q\pi}{2N+1}\right), \quad T_s=\cos\left(\frac{2s-1}{2N+1}\pi\right); \quad q,\ s=1,2,3,......,N. \tag{13}$$

It can be shown that the SIF is

$$K_I=\sqrt{\pi\, l}\,\frac{2\mu_0}{(\kappa_0+1)}\sqrt{2}\varphi_x(+1), \tag{14}$$

where $\varphi_x(+1)$ is computed from Krenk's interpolation formula. The SIFs calculated by above formulations give the approximate values of SIFs for the same crack in the FGM coating as shown in Fig. 1.

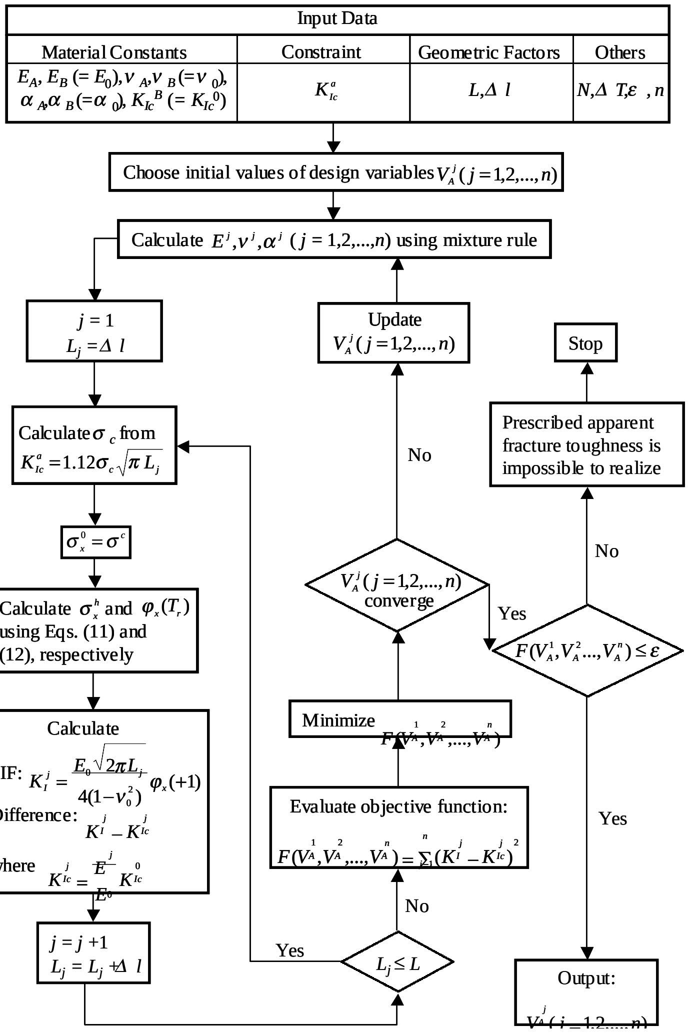

Fig. 4 Flow chart for inverse problem of material distribution to realize prescribed apparent fracture toughness

Table –1 Material properties of TiC and Al_2O_3

Material	Young's Modulus (GPa)	Shear Modulus (GPa)	Poisson's Ratio	CTE (/°C)	K_{Ic} (MPa $m^{1/2}$)
TiC	462	194.12	0.19	7.4×10^{-6}	4.1
Al_2O_3	380	150.79	0.26	8.0×10^{-6}	3.5

Apparent fracture toughness

The SIF at the tip of a crack in homogeneous isotropic materials without any internal stress is expressed in terms of external applied stresses and geometric factors. On the other hand, the SIF at the tip of a crack in FGMs is expressed in terms of not only external applied stresses and geometric factors but also internal stresses and material distributions. For the brittle materials, fracture occurs from the crack tip when the SIF attains the critical value, i.e. the intrinsic fracture toughness. By ignoring the internal stresses and the material distributions in a FGM, let us imagine the FGM with the same geometric configuration under the external applied stress which corresponds to its fracture stress. Then, we can evaluate the critical value of SIF through the formula of SIF for a crack in homogeneous isotropic materials, which is called the apparent fracture toughness of FGMs.

Now we consider an edge crack of length l in the FGM coating bonded to the semi-infinite homogeneous substrate as shown in Fig. 1. When the far-field applied stress at which the fracture occurs from the crack tip is σ_c on the average, the apparent fracture toughness of the FGM coating-substrate system can be given, using the formula of SIF for an edge crack of length l in semi-infinite homogeneous isotropic materials, by

$$K^a_{Ic} = 1.12\sigma_c\sqrt{\pi\, l}\ . \tag{15}$$

Although the far-field applied stress σ^f_x in the FGM coating is non-uniform, we can regard σ_c to be equal to the far-field applied stress acting in the semi-infinite homogeneous substrate because the thickness of the FGM coating is small in comparison with that of the substrate. Therefore, σ_c is given by σ^0_x satisfying

$$K_I = K_{Ic} \tag{16}$$

where K_{Ic} is the intrinsic fracture toughness of the FGM coating.

Inverse analysis of apparent fracture toughness

Suppose that a profile of the apparent fracture toughness K^a_{Ic} is prescribed over a region of distance L measured from the free surface of a FGM coating. To carry out the inverse calculations, the distance L is divided by a large number n so that every small interval ΔL is equal to L/n.. The distances L_j (j = 1,2,…,n) on L are taken as j times

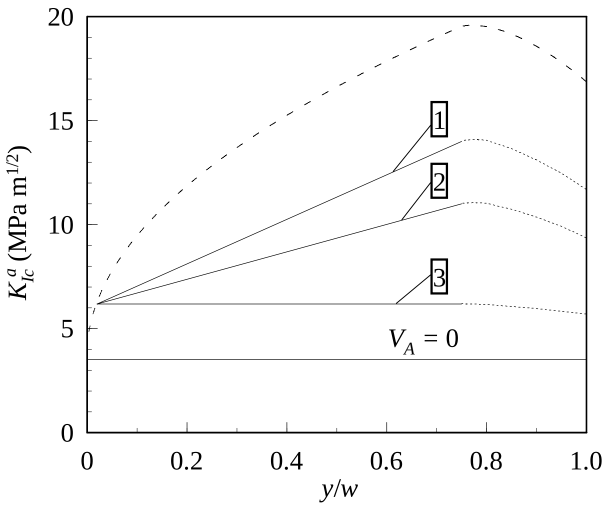

Fig. 5 Prescribed apparent fracture toughness in a TiC/Al_2O_3 FGM coating bonded to a semi-infinite homogeneous substrate of Al_2O_3

ΔL. The volume fraction of constituent A that is assumed to be a constant over $L_{j-1} \le -y \le L_j$ is denoted by V^j_A. Using the volume fractions V^j_A as design variables, the optimization problem of the material distribution profile over the region of distance L in the FGM coating is set up as

$$\text{Minimize}: F(V^1_A, V^2_A, ..., V^n_A) = \sum_{j=1}^{n}\left(K^j_I - K^j_{Ic}\right)^2 \qquad \text{Subject to}: 0 \le V^j_A \le 1;\quad j = 1,2,...,n \tag{17}$$

where K^j_I is the SIF at the crack tip which is located at the point y = -L_j and K^j_{Ic} is the intrinsic fracture toughness on $L_{j-1} \le -y \le L_j$. The material properties E^j, ν^j, α^j and K^j_{Ic}(j = 1,2,…,n) in the FGM coating are evaluated by using the mixture rules [10, 11]. Equation (17) can be solved by using a mathematical programming method. A flow chart describing the minimization procedure of the objective function $F(V^1_A, V^2_A, ..., V^n_A)$ is shown in Fig. 4. After convergence, the minimum value of the objective function is compared with a small positive quantity ε to verify that the solution of the inverse problem is acceptable.

NUMERICAL RESULTS AND DISCUSSION

To obtain numerical results, a TiC/Al_2O_3 FGM coating bonded to a semi-infinite homogeneous substrate of Al_2O_3 is considered in this study as an example. The values of the mechanical and thermal properties of TiC and Al_2O_3 are shown in Table 1. The temperature range ΔT is taken as 1000° C and the thickness w is taken as 1 mm.

Fig. 5 shows the prescribed apparent fracture toughness K_{Ic}^{a} as a function of normalized distance y/w. The broken line in Fig. 5 represents the upper limit of K_{Ic}^{a} obtained for the maximum possible volume fraction of TiC. The line corresponding to $V_A = 0$ represents the intrinsic fracture toughness K_{Ic}^{0} of the substrate of Al_2O_3. The solid portions (y/w = 0.02 to 0.75) of the curves 1, 2 and 3 indicate the prescribed distribution of K_{Ic}^{a} which is assumed as to be higher than K_{Ic}^{0}. For this prescribed apparent fracture toughness, the corresponding material distribution profiles are calculated which are shown

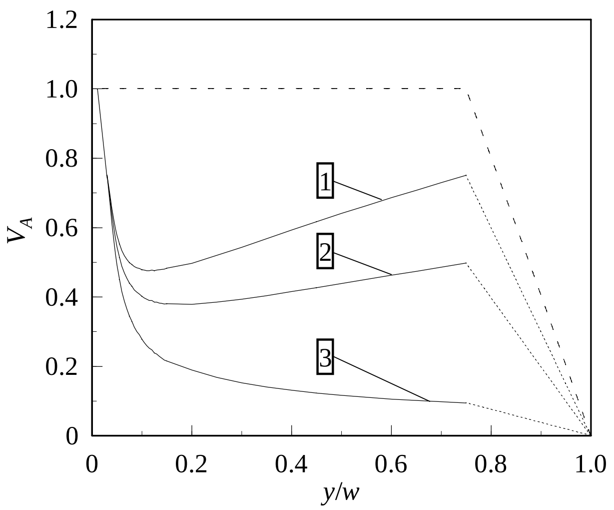

Fig. 6 Material distribution profile of TiC in a TiC/Al_2O_3 FGM coating bonded to a semi-infinite homogeneous substrate of Al_2O_3

by the solid portions of the curves 1,2 and 3 in Fig. 6. The apparent fracture toughness K_{Ic}^{a} over the normalized distance from y/w = 0.75 to 1 as shown by the dotted portions of the curves 1, 2 and 3 in Fig. 5 is calculated for the assumed material distribution profiles shown by the dotted portions of the curves 1, 2 and 3 in Fig. 6. Although the broken line in Fig. 5 represents the upper limit of the apparent fracture toughness K_{Ic}^{a}, it may not be expected that any profiles of the prescribed apparent fracture toughness below this upper limit can be realized within the allowable limits.

The prescribed apparent fracture toughness, considered in all the examples as shown in Fig. 5 is realized by designing the FGM coating having the material distributions shown in Fig. 6. From this fact, it can be concluded that an apparent fracture toughness in FGM coatings bonded to a semi-infinite homogeneous substrate can be controlled within possible limits so as to achieve desired brittle fracture characteristics by choosing an appropriate material distribution in the coatings.

CONCLUSIONS

An inverse method has been developed for optimization of material distribution intending to realize prescribed apparent fracture toughness in FGM coatings. The incompatible eigenstrain induced in the coatings due to mismatch in the coefficients of thermal expansion after cooling from the sintering temperature has also been taken into consideration. An approximation method of calculating SIFs for an edge crack in the FGM coatings subjected to a far field applied load is presented in which the nonhomogeneous material properties of the FGM coatings are simulated by a distribution of equivalent eigenstrain. The approximation method of SIFs is applied to the inverse calculations of material distributions intending to realize prescribed apparent fracture toughness in the coatings. The numerical results are obtained for a TiC/Al_2O_3 FGM coating-Al_2O_3 substrate system which are shown graphically. It can be concluded that the apparent fracture toughness in FGM coatings can be controlled within possible limits so as to achieve desired brittle fracture characteristics by choosing an optimum material distribution in the coating.

REFERENCE

[1] Lannutti, J.J., "Functionally Graded Materials: Properties, Potential and Design Guidelines", *Compos. Eng.*, Vol. 4, 1994, p. 81-94.

[2] Gecit, M.R., "Fracture of a Surface Layer Bonded to a Half Space", *Int. J. Eng. Sci.*, Vol. 17, No. 3, 1979, p. 287-295.

[3] Hu, M.S. and Evans, A.G., "The Cracking and Decohesion of Thin Films on Ductile Substrate", *Acta Metal.*, Vol. 37, No. 3, 1989, p. 917-925.

[4] Makworth, A.J. and Saunders, J.H., "A Model of Structure Optimization for a Functionally Graded Material", *Mater. Lett.*, Vol. 22, No. 1-2, 1995, p. 103-107.

[5] Nadeau, J.C and Ferrai, M., "Microstructural optimization of a fuctionally graded transversely isotropic layer", *Mech Mater.*, Vol. 31 No. 10, 1999, p. 637-651

[6] Nadeau, J.C and Meng, X. N., "On the Response Sensitivity of an Optimally Designed Functionally Graded Layer", *Compos. B*, Vol. 31, No. 4, 2000, p. 285-297.

[7] Nakamura, T., Wang, T. and Sampath, S., "Determination of Properties of Graded Materials by Inverse Analysis and Instrumented Identation",

Acta Mater., Vol. 48, No. 17, 2000, p. 4293-4306.

[8] Sekine, H. and Afsar, A.M., “Composite Profile for Improving the Brittle Fracture Characteristics in Semi Infinite Functionally Graded Materials”, *JSME Int. J.,* Ser. A, Vol. 42, No. 4, 1999, p.592-600.

[9] Afsar, A. M. and Sekine, H., “Crack Spacing Effect on the Brittle Fracture Characteristics of Semi Finite Functionally Graded Materials with Periodic Edge Cracks”, *Int. J.Frac.*, Vol. 102, No. 3, 2000, p.L61-L66

[10] Nan, C.-W., Yuan, R.-Z. and Zhang, L.-M., “The Physics of Metal/Ceramic Functionally Gradient Materials”, Holt, J.B., Koizumi, M., Hirai, T. and Munir, Z.A. editors. *Ceramic Transaction: Functionally gradient materials*, Westerville, Ohio: The American Ceramic Society, Vol. 34, 1993, p. 75-82.

[11] Nair, S.V., “Crack-Wake Debonding and Toughness in Fiber-or Whisker-Reinforced Brittle-Matrix Composites”, *J. Am. Ceram. Soc.*, Vol. 73, No. 10, 1990, p. 2839-2847.